Self-organized spiral patterns at the edge of an order-disorder nonequilibrium phase transition

Italo'Ivo Lima Dias Pinto ⬤

US DEVCOM Army Research Laboratory, Human Research and Engineering Directorate, Aberdeen Proving Ground, Maryland 21005, USA

Daniel Escaff ⬤

Universidad de los Andes, Chile. Facultad de Ingeniería y Ciencias Aplicadas, Av. Monseñor Alvaro del Portillo 12.455 Las Condes, Santiago, Chile

Alexandre Rosas

Departamento de Física, CCEN, Universidade Federal da Paraíba, Caixa Postal 5008, 58059-900, João Pessoa, Paraíba, Brazil

We present a spatially extended version of the Wood–Van den Broeck–Kawai–Lindenberg stochastic phase-coupled oscillator model. Our model is embedded in two-dimensional (2d) array with a range-dependent interaction. The Wood–Van den Broeck–Kawai–Lindenberg model is known to present a phase transition from a disordered state to a globally oscillatory phase in which the majority of the units are in the same discrete phase. Here we address a parameter combination in which such global oscillations are not present. We explore the role of the interaction range from a nearest neighbor coupling in which a disordered phase is observed and the global coupling in which the population concentrate in a single phase. We find that for intermediate interaction range the system presents spiral wave patterns that are strongly influenced by the initial conditions and can spontaneously emerge from the stochastic nature of the model. Our results present a spatial oscillatory pattern not observed previously in the Wood–Van den Broeck–Kawai–Lindenberg model and are corroborated by a spatially extended mean-field calculation.

I. INTRODUCTION

The study of discrete state stochastic oscillators has received a great deal of attention in the past decade. This kind of systems is used to model a wide range of different systems. We can highlight numerous studies that present models in which a network of coupled oscillators undergoes a phase transition to a synchronized phase when the coupling strength exceeds a certain threshold; see, for instance, Refs. [1–12].

A specific model of three state oscillators exhaustively studied by Wood and collaborators [9–12], referred here as the Wood–Van den Broeck–Kawai–Lindenberg model, is composed by oscillators coupled by the transition rates that depends on the number of units in each state. A phase transition from a disordered phase to a synchronized phase was fully characterized for this system. Afterward, it was shown that this model presents a second transition from the synchronized phase to a phase in which the system is dominated by one state with a few units on the other states [13,14]. Most of these results focused on a globally coupled system and the effects of fluctuations due to finite numbers [15]. More recently, we explored the effects of a nonlocal coupling on a one-dimensional array. With this coupling, the system presents very rich dynamics with not only disordered and synchronized phases but also the formation of traveling waves [16].

In this paper, we focus on a two-dimensional system with nonlocal interactions that presents a rich variety of spatial patterns. Our system is a two-dimensional lattice of three state oscillators with unidirectional transitions governed by Markov processes. The transition rates of each unit presents a dependence on the states of all the units in the neighborhood. Here we set the interaction parameter value (corresponding to the phase dominated by a single state in the globally coupled model) and explore the range of the neighborhood. For a small interaction range the oscillators interact with only a few other oscillators and a disordered state emerges, while a middle range interaction leads to the formation of circular waves with spiral-like sources, and for large interaction ranges a coarsening transient occurs that leads the system to a state in which almost the entire population of oscillators are in the same state; this behavior is in agreement with results for the global coupled system.

The paper is organized as follows: In Sec. II, we describe our model. In Secs. III and IV, we present results obtained from numerical simulations. In Sec. V, we present a mean-field approach to the investigated model. In Sec. VI, we present our conclusions.

II. MODEL

Inspired by the work of Wood [9–12], in this paper we explore a set of Markovian three-state stochastic oscillators with unidirectional transitions as in the schematic picture of Fig. 1, arranged in a two-dimensional lattice. This particular model of stochastic oscillator recently gained attention for
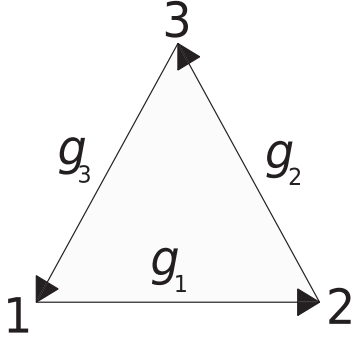
FIG. 1. Schematic picture of a three-state stochastic oscillator with unidirectional transitions.

being one of the simplest models of discrete-state stochastic oscillators that undergo a transition to a synchronized state.

As in the Wood–Van den Broeck–Kawai–Lindenberg model of three-state stochastic oscillators, the transition rates depend on the density of units in each state. For our model, we also take into account the spatial distribution of the units and we define the transition rates as

$$g_i = \exp\left[a(v_{i+1} - v_i)\right], \tag{1}$$

in which g_i represents the rate of the transition for a unit in state i to the state $i + 1$, a is the coupling parameter and controls how strong is the coupling between the units, and v_i is the density of units in the state i weighted by the kernel f_σ. Hence, we can write v_i as

$$v_i(\vec{r}, t) = \sum_{\vec{r}' \in \Omega} f_\sigma(\vec{r}') s_i(\vec{r} + \vec{r}', t), \tag{2}$$

where $\vec{r}$ is the position vector of a given unit, Ω is the set of $\vec{r}$ for all units in the array, and s_i is 1 if the unit is in state i and 0 if the unit is in any other state. By the use of the convolution theorem, this computation can be done considerably more quickly, as discussed in the Appendix. For our simulations, we used the interaction kernel $f_\sigma(\vec{r})$ as

$$f_\sigma(\vec{r}) = \begin{cases} N_n, & \text{for } |\vec{r}| < \sigma \\ \frac{N_n}{2}, & \text{for } |\vec{r}| = \sigma, \\ 0, & \text{for } |\vec{r}| > \sigma \end{cases} \tag{3}$$

where N_n is a normalization constant that confines v_i to the interval between 0 and 1. In our model, we use periodic boundary conditions, and we always consider σ smaller than half the length of the system, not counting the contribution of each oscillator for v_s twice.

III. SPIRAL-LIKE STRUCTURES AT THE EDGE OF AN ORDER-DISORDER NONEQUILIBRIUM PHASE TRANSITION

It is well known that the Wood–Van den Broeck–Kawai–Lindenberg model presents a phase transition to a synchronized oscillatory state in which most of the oscillators cycle through the three discrete states in unison [10–12]. This transition to the synchronized phase is well explored; the critical point occurs for the coupling parameter $a_c = 1.5$, with the synchronized phase occurring for strong coupling and a

disordered phase for weak coupling [9]. Further increase in the coupling parameter can induce a second phase transition with a critical point $a^c \approx 3.1$. This second transition occurs between a globally oscillatory phase and an ordered phase in which the system gets "stuck" with almost all units in the same state [13]. From the bifurcation diagram of the mean-field dynamical equations, an infinite period bifurcation [17] can be observed; this bifurcation disrupts the synchronized state, generating three symmetric ordered states.

Characterization of the transition from the disordered to oscillatory phase in a locally coupled lattice shows that this phase transition presents signatures of the XY universality class [9] with a lower critical dimension $d_{lc} = 2$ and upper critical dimension $d_{lc} = 4$, such that no synchronized phase is observed for the two-dimensional locally coupled case.

In our simulations, we used a square lattice with periodic boundary conditions. The coupling parameter was kept constant, $a = 3.5$, such that even in the global coupling limit ($\sigma \to L$) the global oscillations are absent. We explored the effect of interaction range and how the system behaves on this route from a disordered phase observed for nearest neighbor interaction and an ordered phase with the global coupling.

Results from the stochastic simulation of this arrangement are summarized in Fig. 2. We could observe three kinds of dynamics shown on the three top panels of Fig. 2: On the left panel is the nearest neighbor ($\sigma = 1$) case, showing a disordered phase with no distinguishable pattern. In the middle panel is shown the case with a "medium interaction range" ($\sigma = 3.5$) with a clear spiral-like wave pattern; in this regime, the system presents interesting dynamics with spiral-like structures circulating and generating the waves [18]. On the right panel, we present a snapshot for sufficiently long-range interactions ($\sigma = 7$); in this case the ordered phase arises and most units are "frozen" in the same phase.

In order to identify the phase transition to the ordered phase, we use the Kuramoto order parameter [19,20] defined as

$$re^{i\psi} = \frac{1}{N} \sum_{j=1}^{N} e^{i\theta_j}, \tag{4}$$

in which θ_j is the phase of the oscillator j, taken to be $2\pi\left(\frac{k-1}{3}\right)$, where k is the state of oscillator j, and in our case $k \in \{1, 2, 3\}$. This complex order parameter tells us the average phase of the population ψ and the amplitude r measures the coherence of the population. For the specific case of three discrete states, $r = 0$ (disordered phase) if the oscillators are evenly distributed in the states. In the case that all the population is concentrated in a given state, $r = 1$ (ordered phase).

On the bottom panel of Fig. 2 we present r as a function of σ; these results were obtained from the following simulation scheme: We started from a homogeneous condition (all units in the same state) with $\sigma = 1$ and we evolve the dynamics for a long time (2×10^4 time steps); after this long time evolution we change the σ value and use the final state as the starting condition. We used this scheme for an increasing σ (points linked by continuous lines) and for decreasing σ (points linked by dashed lines).

We used three lattice sizes of side, $L = 128$ (red circles), $L = 256$ (blue triangles), and $L = 512$ (green diamonds).
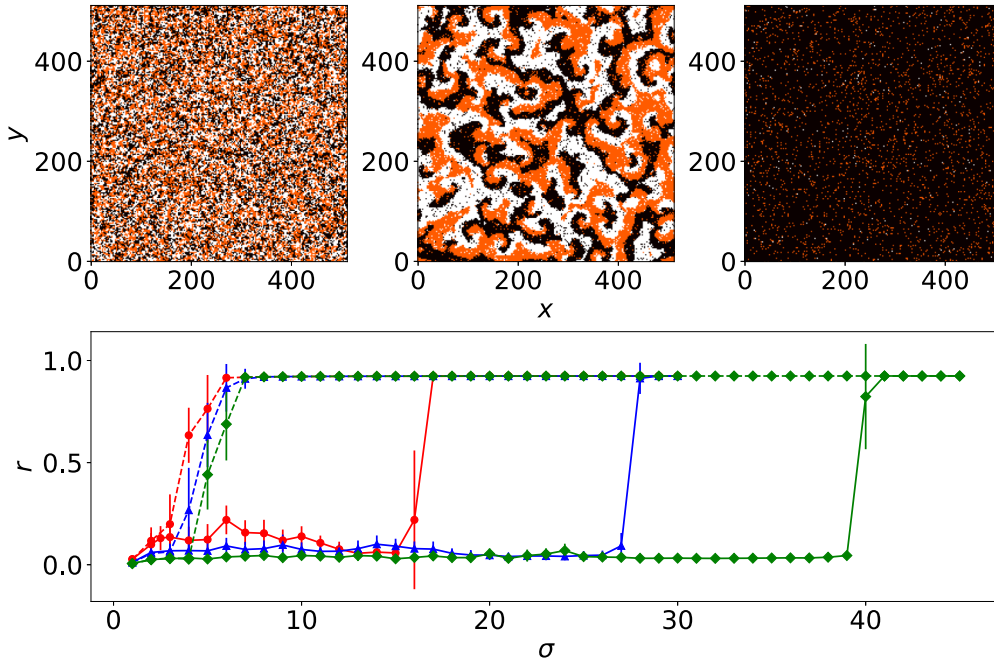
FIG. 2. Top: Snapshots of the steady state for three different interaction ranges with $L = 512$. $\sigma = 1$ in the left panel, $\sigma = 3.5$ in the middle panel, and $\sigma = 7$ on the right panel. On the bottom, we present the Kuramoto order parameter as a function of the interaction range σ. Here we explored lattices with different sizes $L = 128$ (red circles), 256 (blue triangles), and 512 (green diamonds). We use the final state for each σ value as the initial condition for the next one; we denote increasing σ with points linked by a continuous line and decreasing σ with points linked by dashed lines.

This simulation scheme clearly shows a coexistence region in which the system presents spiral-like wave patterns (Fig. 2, top middle panel) and the ordered phase (Fig. 2, top right panel), depending on the initial conditions. For decreasing σ, we observe a decay in r associated with the formation of the spiral-like wave pattern for $\sigma \approx 5$ independent of lattice size. For increasing σ, a sharp increase in r associated with the ordered phase occurs for different values of σ depending on lattice size such that the coexistence is observed in a larger range of σ for larger lattices. It is important to note that the spiral-like wave pattern is characterized by $r \approx 0$ being on the edge of the transition to the ordered state. It is also worth noting that the area between hysteresis curves can be affected by the cooling time between the adjustments on the control parameter σ; to obtain the bottom panel of Fig. 2 a long cooling time was used, such that a slight decrease was observed for $L = 128$ using a cooling time twice as long. For the larger values of L, no difference of the area between the hysteresis curves was observed as we doubled the cooling time.

Further investigation shows that the spiral-like wave patterns increase in size as we increase σ, as shown on Fig. 3. On the left panel, we can observe the pattern obtained for $\sigma = 4$: The system always evolves to sustain such pattern independent of the initial conditions. On the middle panel, we can observe that the spiral-like structures on the pattern are large. This state can only be obtained if the system presents a nonhomogeneous initial condition; it does not emerge for an homogeneous initial condition as can be observed on the lower panel of Fig. 2. On the right panel of Fig. 3, we observe the pattern for $\sigma = 20$; in such a case, only a single stable spiral-like structure is observed. For sufficiently large σ,

the lattice does not support the existence of the central spiral-like structure, since the generated wave interacts with the central spiral-like structure.

We can observe that r assumes low values for local coupling; for sufficiently long-range interactions the ordered phase (high value of r) is observed. This was expected since it reproduces the two-dimensional local coupling limit and the global coupling [10].

For very short interaction range ($\sigma < 3$), a disordered state such as presented in top left panel of Fig. 2 is observed; the spiral-like pattern spontaneously emerges for $\sigma \approx 3$ independent of the initial conditions. As we increase the interaction range ($\sigma \approx 5$), the spiral-like pattern emergence becomes strongly dependent on the initial conditions.

This dependence can be explained as following: For short-range interactions, a small pattern is required to support the emergence of vortex-like structures; this pattern can emerge spontaneously due to the stochastic nature of the units. As the interaction range increases, a larger pattern is required to support the existence of the spiral-like structures. In our simulation scheme for Fig. 2, we use the final state of the previous value of σ as the initial state for the next simulation (with different value of sigma). For the case in which the simulation starts with an already existing spiral-like pattern, the spiral-like structures tend to persist (increasing σ simulations). For the case of an absence of spiral-like structures in the initial state, the emergence of the spiral-like structures occurs only for short-range interactions (decreasing σ simulations).

The above description is corroborated by our mean-field analysis in the Sec. V.
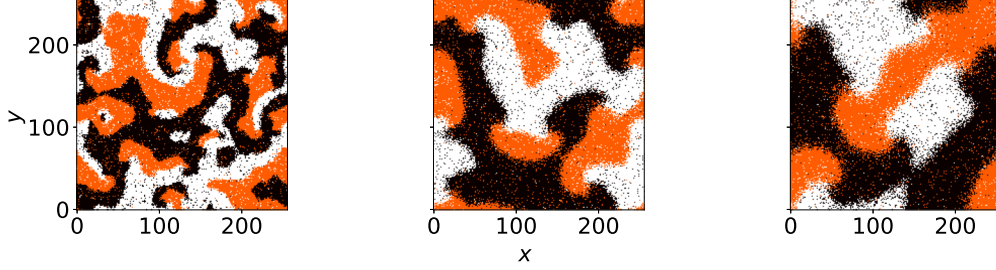
FIG. 3. Snapshots of the spiral-like pattern in three different interaction ranges: $\sigma = 4$ in the left panel, $\sigma = 10$ in the middle panel, and $\sigma = 20$ on the right panel. The lattice size is $L = 256$.

IV. MAXIMUM SYNCHRONIZED CLUSTER SIZE AS AN INDICATIVE OF EXISTENCE OF SPIRAL-LIKE STRUCTURES

Since the Kuramoto order parameter fails to identify the emergence of spiral-like structures, we propose the maximum size of a cluster of synchronized units for such, and it is formally defined as

$$c_{\max} = \langle 3(n_{1\max}n_{2\max}n_{3\max})^{1/3}\rangle, \tag{5}$$

where $n_{k\max} = \frac{N_{k\max}}{N}$, with $N_{k\max}$ being the largest cluster in state k, N is the total number of lattice sites, and $\langle.\rangle$ denotes a temporal mean. In the synchronized region, the largest clusters of the three populations are all large, so $c_{\max}$ is large, while $c_{\max}$ is small either if all clusters are small or even if one or two clusters are large as long as at least one cluster is small. The factor 3 is a normalization factor so that the maximum value of $c_{\max}$ is 1 (there is only one cluster of each population and the clusters are of the same size, so that $n_{1\max} = n_{2\max} = n_{3\max} = 1/3$).

Figure 4 presents $c_{\max}$ calculated for lattices of different sizes; the same simulation scheme used in Fig. 2 was used here. The same color code used for Fig. 2 was used here with $L = 128$ (red circles), $L = 256$ (blue triangles), and $L = 512$ (green diamonds) with continuous (dashed) line indicating the increasing (decreasing) σ. The $c_{\max}$ measurement can detect the presence of spiral-like structures in the system; observe that $c_{\max}$ increases for values of σ in which spiral-like structures are observed and rapidly vanishes for values of σ in which spiral-like structure collapses and only the ordered state is observed. Using $c_{\max}$ and the Kuramoto order

parameter, one can determine in which phase a given lattice is observed. If both are 0, the system is in a disordered state; if $r = 0$ and $c_{\max} > 0$, spiral-like structures are present; and if both $r > 0$ and $c_{\max} = 0$, the system is in the ordered phase.

V. MEAN-FIELD APPROACH

We have also explored the appearance of all this type of waving patterns in the mean-field (noiseless) version of the model. In order to do a mean-field analysis for this model, we start with the master equation for the probability $p_i(\vec{k}, t)$ that a unit on the position $\vec{k}$ of the lattice is in state i at time t. Also, we have the probability normalization condition, expressed by $p_1(\vec{k}, t) + p_2(\vec{k}, t) + p_3(\vec{k}, t) = 1$; using this condition, we can obtain the probability dynamics from only two equations:

$$\dot{p}_1(\vec{k}, t) = g_3(\vec{k}, t) - [g_1(\vec{k}, t) + g_3(\vec{k}, t)]p_1(\vec{k}, t)$$
$$- g_3(\vec{k}, t)p_2(\vec{k}, t), \tag{6}$$
$$\dot{p}_2(\vec{k}, t) = -g_2(\vec{k}, t)p_2(\vec{k}, t) + g_1(\vec{k}, t)p_1(\vec{k}, t),$$

with $g_i(\vec{k}, t)$ defined by Eq. (1) and $p_i(\vec{k}, t)$ as the probability of finding a unit in state i in position $\vec{k}$ at time t.

We can solve this system using the mean-field approximation, relating s_i with the probabilities p_i:

$$v_i(\vec{k}, t) \approx \langle v_i(\vec{k}, t)\rangle = \sum_{\Omega} f_\sigma(\vec{k}')p_i(\vec{k} + \vec{k}', t). \tag{7}$$

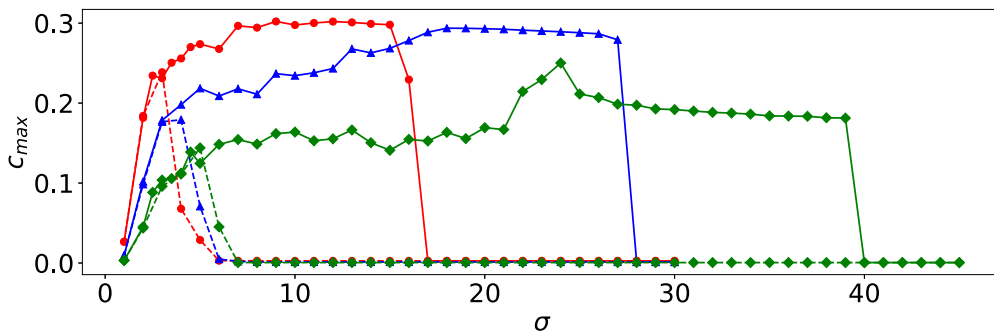Observe that the normalization constant N_n keeps v_i bounded between 0 and 1.

FIG. 4. Maximum synchronized cluster size as a function of the interaction range σ. Here we explored lattices with different sizes $L = 128$ (red circles), 256 (blue triangles), and 512 (green diamonds). Unlike the Kuramoto order parameter, this new parameter allows the detection of spiral-like structures, being zero when spiral-like structures are absent.
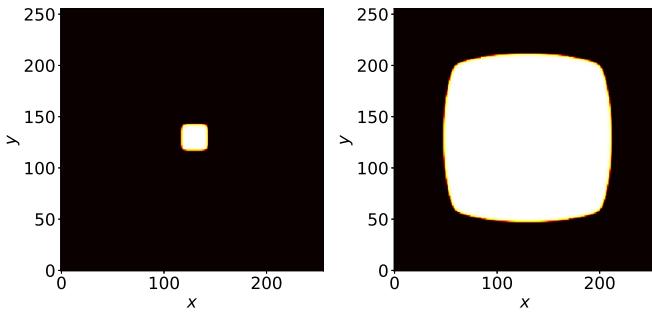
FIG. 5. Snapshots of the initial condition and the evolution to the steady state for the solution of the mean-field equations ($\sigma = 1$).

Equations (6) can be solved numerically using the mean-field approximation (7).

In our numerical solution, a 256×256 lattice was used, and at each point of the lattice we integrated the differential equations for $p_1(\vec{k}, t)$ and $p_2(\vec{k}, t)$ using a fourth-order Runge-Kutta algorithm. Observe that this approach allows us to investigate the evolution of the system without any noise, intrinsic to the stochastic nature of the model. In this case, the steady state is highly sensitive to the initial conditions for $p_1(\vec{k}, t)$ and $p_2(\vec{k}, t)$. This fact is corroborated by Figs. 5 and 6; both figures were obtained from the solution of the mean-field equations with $\sigma = 1$, and the left panel of each figure shows the initial condition for each case [18].

In Fig. 5, the initial condition is an homogeneous square in the center of the lattice; as the system evolves, this homogeneous domain increases (right panel) and dominates the whole lattice, resulting in the ordered phase in the transient regime. This result shows that the disordered state in the stochastic simulations occur due to the random nature of the oscillators associated with the short-range interaction (fewer units interacting results in larger fluctuations) [15].

In Fig. 6, the initial condition is a small spiral-like structure in the center of the lattice; for this case, the system evolves, generating a stable spiral-like structure. The steady state of the system develops such that traveling waves are observed generated by the central spiral-like structure; a snapshot of this steady state is shown in the right panel of Fig. 6. For higher values of σ, larger spiral-like structures as initial conditions are needed to maintain the central spiral-like structure, and larger spiral-like patterns are observed at the steady state.

These mean-field results support the dynamics observed from the stochastic simulations. When we have small values
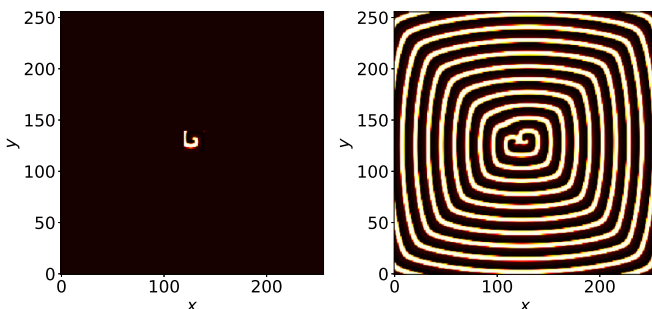
of σ, the random nature of the units dominates and only a disordered phase is observed; as σ increases, small spiral-like structures spontaneously appear and persist as stable structures. Once we have a spiral-like pattern formed either by noise or set as an initial condition, it is stable and persists for long periods. For larger σ, the spiral-like structures are larger, up to the point that they interact with themselves due to the periodic boundary conditions and get annihilated. In the case where the initial condition is homogeneous, the spiral-like structures appear only when the interaction range is short enough to allow the central pattern of the spiral-like structure to spontaneously appear as a result of fluctuations (in this case, the emergence of the spiral-like structures depends on σ and not on the lattice size).

VI. CONCLUSIONS

In this paper, we study the Wood–Van den Broeck–Kawai–Lindenberg model of discrete phase-coupled oscillators, in which each oscillator has three discrete phases and cycles through them in an unidirectional way. Our model departs from the original Wood–Van den Broeck–Kawai–Lindenberg model by the inclusion of an interaction range parameter σ on a two-dimensional lattice. The interaction range parameter is such that in the case of only nearest neighbor interaction $\sigma = 1$ and the interaction range increases as σ increases.

This model presents a disordered phase dominated by noise for the limit of nearest neighbor interaction; as we increase the interaction range spiral-like waves are observed and for larger values of σ larger spiral-like patterns emerge. Despite the large spiral-like structures observed for large values of σ, the spiral-like structures only emerge spontaneously for small values of σ as an interplay of noise and the small pattern necessary for the spiral-like structure formation. For a very large interaction range, the spiral-like waves interfere with themselves and cease to be stable; in such a limit, we observe an ordered phase regime. Our analyses were done through simulation of the stochastic model and are corroborated by mean-field calculations.

Our results presents a spatial oscillatory pattern not observed previously on the Wood–Van den Broeck–Kawai–Lindenberg model. The oscillatory pattern occurs at the onset of a order-disorder transition in which the interaction range acts as a control parameter. It is important to observe that the spiral-like patterns observed does not represent global oscillations, in the sense that the system still presents $\frac{1}{3}$ of the population in each discrete phase.

FIG. 6. Snapshots of the initial condition and the evolution to the steady state for the solution of the mean-field equations ($\sigma = 1$).

and should not be interpreted as representing the official policies, either expressed or implied, of the Army Research Laboratory or the U.S. Government. The U.S. Government is authorized to reproduce and distribute reprints for Government purposes notwithstanding any copyright notation herein.

APPENDIX

In order to speed up the computational simulations presented in this paper, we took advantage of the discrete convolution theorem. In the discrete version of the convolution theorem, the convolution of x and y is defined as

$$x * y = \sum_{m=0}^{N-1} x_N(m) y_N(n-m), \tag{A1}$$

in which case x_N and y_N denote summation sequences. It is important to notice here the resemblance of the above definition with Eq. (2). The convolution theorem states that

$$\mathcal{F}(x * y) = \mathcal{F}(x)\mathcal{F}(y). \tag{A2}$$

In order to speed up the calculation of the transition probabilities, one can take advantage of the convolution theorem and use the fast Fourier transform algorithm to calculate the values of ν_i. This method can speed up the calculation of the transition probabilities significantly.

[1] M. Kuperman and G. Abramson, Phys. Rev. Lett. **86**, 2909 (2001).

[2] D. H. Zanette, Phys. Rev. E **64**, 050901(R) (2001).

[3] D. H. Zanette and M. Kuperman, Phys. A (Amsterdam, Neth.) **309**, 445 (2002).

[4] G. Szabó, A. Szolnoki, and R. Izsák, J. Phys. A: Math. Gen. **37**, 2599 (2004).

[5] G. Szabó and G. Fath, Phys. Rep. **446**, 97 (2007).

[6] A. Efimov, A. Shabunin, and A. Provata, Phys. Rev. E **78**, 056201 (2008).

[7] N. Kouvaris, A. Provata, and D. Kugiumtzis, Phys. Lett. A **374**, 507 (2010).

[8] A. Shabunin and A. Provata, Eur. Phys. J. Special Topics **222**, 2547 (2013).

[9] K. Wood, C. Van den Broeck, R. Kawai, and K. Lindenberg, Phys. Rev. Lett. **96**, 145701 (2006).

[10] K. Wood, C. Van den Broeck, R. Kawai, and K. Lindenberg, Phys. Rev. E **74**, 031113 (2006).

[11] K. Wood, C. Van den Broeck, R. Kawai, and K. Lindenberg, Phys. Rev. E **75**, 041107 (2007).

[12] K. Wood, C. Van den Broeck, R. Kawai, and K. Lindenberg, Phys. Rev. E **76**, 041132 (2007).

[13] V. R. V. Assis, M. Copelli, and R. Dickman, J. Stat. Mech. (2011) P09023.

[14] V. R. Assis and M. Copelli, Phys. A (Amsterdam, Neth.) **391**, 1900 (2012).

[15] Italo'Ivo Lima Dias Pinto, D. Escaff, U. Harbola, A. Rosas, and K. Lindenberg, Phys. Rev. E **89**, 052143 (2014).

[16] D. Escaff, Italo'Ivo Lima Dias Pinto, and K. Lindenberg, Phys. Rev. E **90**, 052111 (2014).

[17] S. H. Strogatz, *Nonlinear Dynamics and Chaos: With Applications to Physics, Biology, Chemistry, and Engineering* (Addison-Wesley, Reading, MA, 1997).

[18] See Supplemental Material at http://link.aps.org/supplemental/10.1103/PhysRevE.103.052215 for videos.

[19] Y. Kuramoto (eds.), *Chemical Oscillations, Waves, and Turbulence* (Dover, Berlin, 1984).

[20] S. H. Strogatz, Phys. D (Amsterdam, Neth.) **143**, 1 (2000).